Check for updates

An infectious SARS-CoV-2 B.1.1.529 Omicron virus escapes neutralization by therapeutic monoclonal antibodies

Laura A. VanBlargan [1], John M. Errico [2], Peter J. Halfmann[3], Seth J. Zost [4,5], James E. Crowe Jr. [4,5,6], Lisa A. Purcell[7], Yoshihiro Kawaoka [3,8,9], Davide Corti [10], Daved H. Fremont [2,11,12] and Michael S. Diamond [1,2,11,13,14] ✉

The emergence of the highly transmissible B.1.1.529 Omicron variant of severe acute respiratory syndrome coronavirus 2 (SARS-CoV-2) is concerning for antibody countermeasure efficacy because of the number of mutations in the spike protein. In this study, we tested a panel of anti-receptor-binding domain monoclonal antibodies (mAbs) corresponding to those in clinical use by Vir Biotechnology (S309, the parent mAb of VIR-7831 (sotrovimab)), AstraZeneca (COV2-2196 and COV2-2130, the parent mAbs of AZD8895 and AZD1061), Regeneron (REGN10933 and REGN10987), Eli Lilly (LY-CoV555 and LY-CoV016) and Celltrion (CT-P59) for their ability to neutralize an infectious B.1.1.529 Omicron isolate. Several mAbs (LY-CoV555, LY-CoV016, REGN10933, REGN10987 and CT-P59) completely lost neutralizing activity against B.1.1.529 virus in both Vero-TMPRSS2 and Vero-hACE2-TMPRSS2 cells, whereas others were reduced (COV2-2196 and COV2-2130 combination, ~12-fold decrease) or minimally affected (S309). Our results suggest that several, but not all, of the antibodies in clinical use might lose efficacy against the B.1.1.529 Omicron variant.

Since December 2019, the global Coronavirus Disease 2019 (COVID-19) pandemic caused by SARS-CoV-2 has resulted in 298 million infections and 5.4 million deaths. The expansion of the COVID-19 pandemic and its accompanying morbidity, mortality and destabilizing socioeconomic effects have made the development and distribution of SARS-CoV-2 therapeutics and vaccines an urgent global health priority[1]. Although the rapid deployment of countermeasures, including mAbs and multiple highly effective vaccines, has provided hope for curtailing disease and ending the pandemic, this has been jeopardized by the emergence of more transmissible variants with mutations in the spike protein that also could evade protective immune responses.

Indeed, over the past year, several variant strains have emerged, including B.1.1.7 (Alpha), B.1.351 (Beta), B.1.1.28 (also called P.1, Gamma) and B.1.617.2 (Delta), among others, each having varying numbers of substitutions in the N-terminal domain (NTD) and the receptor-binding domain (RBD) of the SARS-CoV-2 spike. Cell-based assays with pseudoviruses or authentic SARS-CoV-2 strains suggest that neutralization by many Emergency Use Authorization (EUA) mAbs might be diminished against some of these variants, especially those containing mutations at positions L452, K477 and E484 (refs. [2–6]). Notwithstanding this, in vivo studies in animals showed that, when most EUA mAbs were used

in combination, they retained efficacy against different variants[7]. The recent emergence of B.1.1.529, the Omicron variant[8,9], which has a larger number of mutations (>30 substitutions, deletions or insertions) in the spike protein, has raised concerns that this variant will escape from protection conferred by vaccines and therapeutic mAbs.

Results

We obtained an infectious clinical isolate of B.1.1.529 from a symptomatic individual in the United States (hCoV-19/USA/WI-WSLH-221686/2021). We propagated the virus once in Vero cells expressing human transmembrane protease serine 2 (TMPRSS2) to prevent the emergence of adventitious mutations at or near the furin cleavage site in the spike protein[10]. Our B.1.1.529 isolate encodes the following mutations in the spike protein (A67V, Δ69–70, T95I, G142D, Δ143-145, Δ211, L212I, insertion 214EPE, G339D, S371L, S373P, S375F, K417N, N440K, G446S, S477N, T478K, E484A, Q493R, G496S, Q498R, N501Y, Y505H, T547K, D614G, H655Y, N679K, P681H, N764K, D796Y, N856K, Q954H, N969K and L981F; Fig. 1a,b and GISAID: EPI_ISL_7263803), which is similar to strains identified in Africa[11]. Our isolate, however, lacks an R346K mutation, which is present in a minority (~8%) of reported strains.

[1]Department of Medicine, Washington University School of Medicine, St. Louis, MO, USA. [2]Department of Pathology & Immunology, Washington University School of Medicine, St. Louis, MO, USA. [3]Influenza Research Institute, Department of Pathobiological Sciences, School of Veterinary Medicine, University of Wisconsin-Madison, Madison, WI, USA. [4]Vanderbilt Vaccine Center, Vanderbilt University Medical Center, Nashville, TN, USA. [5]Department of Pediatrics, Vanderbilt University Medical Center, Nashville, TN, USA. [6]Department of Pathology, and Microbiology and Immunology, Vanderbilt University Medical Center, Nashville, TN, USA. [7]Vir Biotechnology, St. Louis, MO, USA. [8]Division of Virology, Department of Microbiology and Immunology, Institute of Medical Science, University of Tokyo, Tokyo, Japan. [9]The Research Center for Global Viral Diseases, National Center for Global Health and Medicine Research Institute, Tokyo, Japan. [10]Humabs BioMed SA, a subsidiary of Vir Biotechnology, Bellinzona, Switzerland. [11]Department of Molecular Microbiology, Washington University School of Medicine, St. Louis, MO, USA. [12]Department of Biochemistry & Molecular Biophysics, Washington University School of Medicine, St. Louis, MO, USA. [13]Andrew M. and Jane M. Bursky Center for Human Immunology and Immunotherapy Programs, Washington University School of Medicine, St. Louis, MO, USA. [14]Center for Vaccines and Immunity to Microbial Pathogens, Washington University School of Medicine, St. Louis, MO, USA. ✉e-mail: mdiamond@wustl.edu
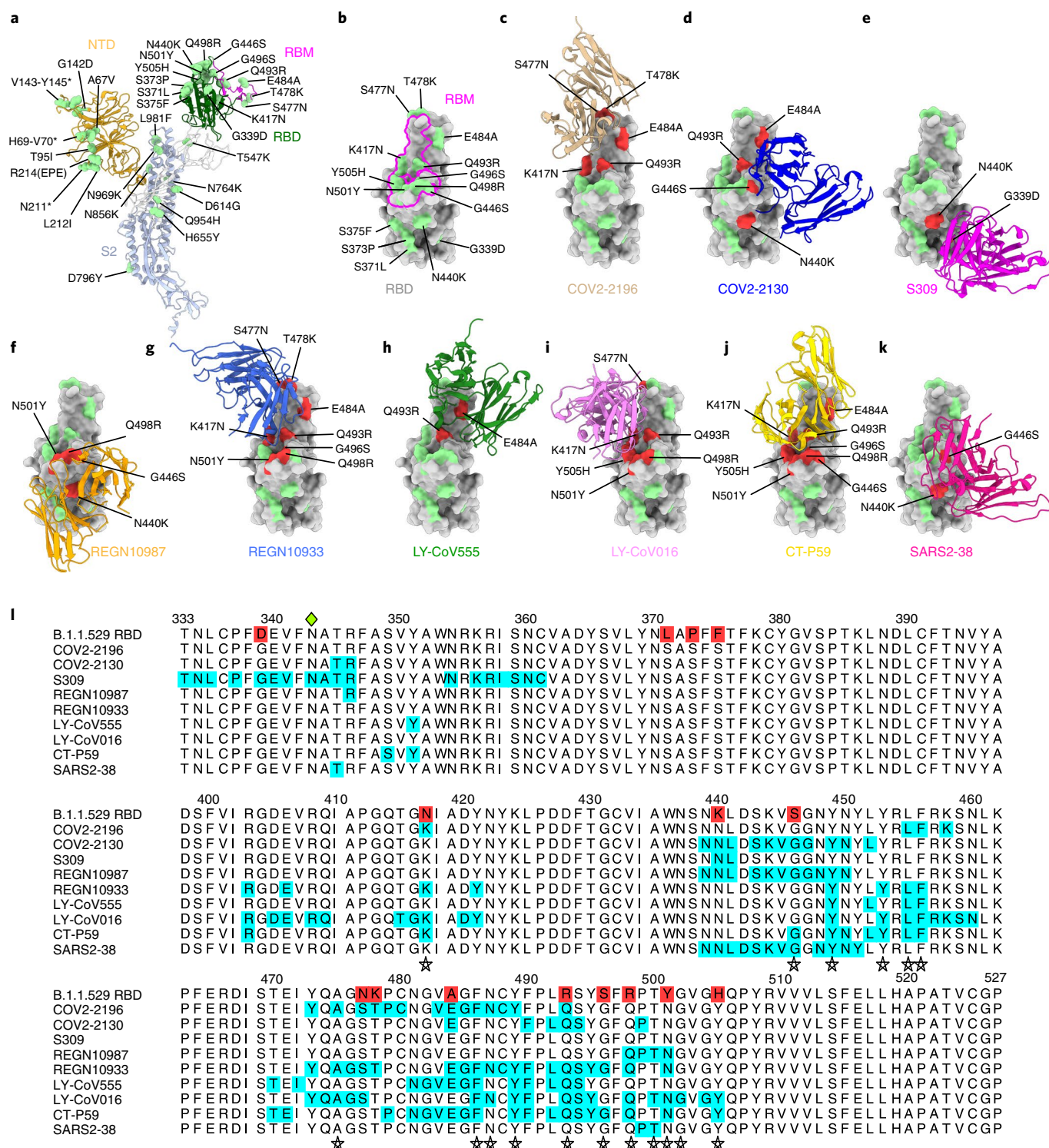
Fig. 1 | Neutralizing mAb epitopes on B.1.1.529. a, **b**, SARS-CoV-2 spike trimer (PDB: 7C2L and PDB: 6W41). One spike protomer is highlighted, showing the NTD in orange, RBD in green, RBM in magenta and S2 portion of the molecule in blue (**a**). Close-up view of the RBD with the RBM outlined in magenta (**b**). Amino acids that are changed in B.1.1.529 compared to WA1/2020 are indicated in light green (**a**, **b**), with the exception of N679K and P681H, which were not modeled in the structures used. **c–k**, SARS-CoV-2 RBD bound by EUA mAbs COV2-2196 (**c**, PDB: 7L7D); COV2-2130 (**d**, PDB: 7L7E); S309 (**e**, PDB: 6WPS); REGN10987 (**f**, PDB: 6XDG); REGN10933 (**g**, PDB: 6XDG); LY-CoV555 (**h**, PDB: 7KMG); LY-CoV016 (**i**, PDB: 7C01); CT-P59 (**j** PDB: 7CM4); and SARS2-38 (**k**, PDB: 7MKM). Residues mutated in the B.1.1.529 RBD and contained in these mAbs' respective epitopes are shaded red, whereas those outside the epitope are shaded green. **l**, Multiple sequence alignment showing the epitope footprints of each EUA mAb on the SARS-CoV-2 RBD highlighted in cyan. B.1.1.529 RBD is shown in the top row, with sequence changes relative to the wild-type RBD highlighted red. A green diamond indicates the location of the N-linked glycan at residue 343. Stars below the alignment indicate hACE2 contact residues on the SARS-CoV-2 RBD[40].
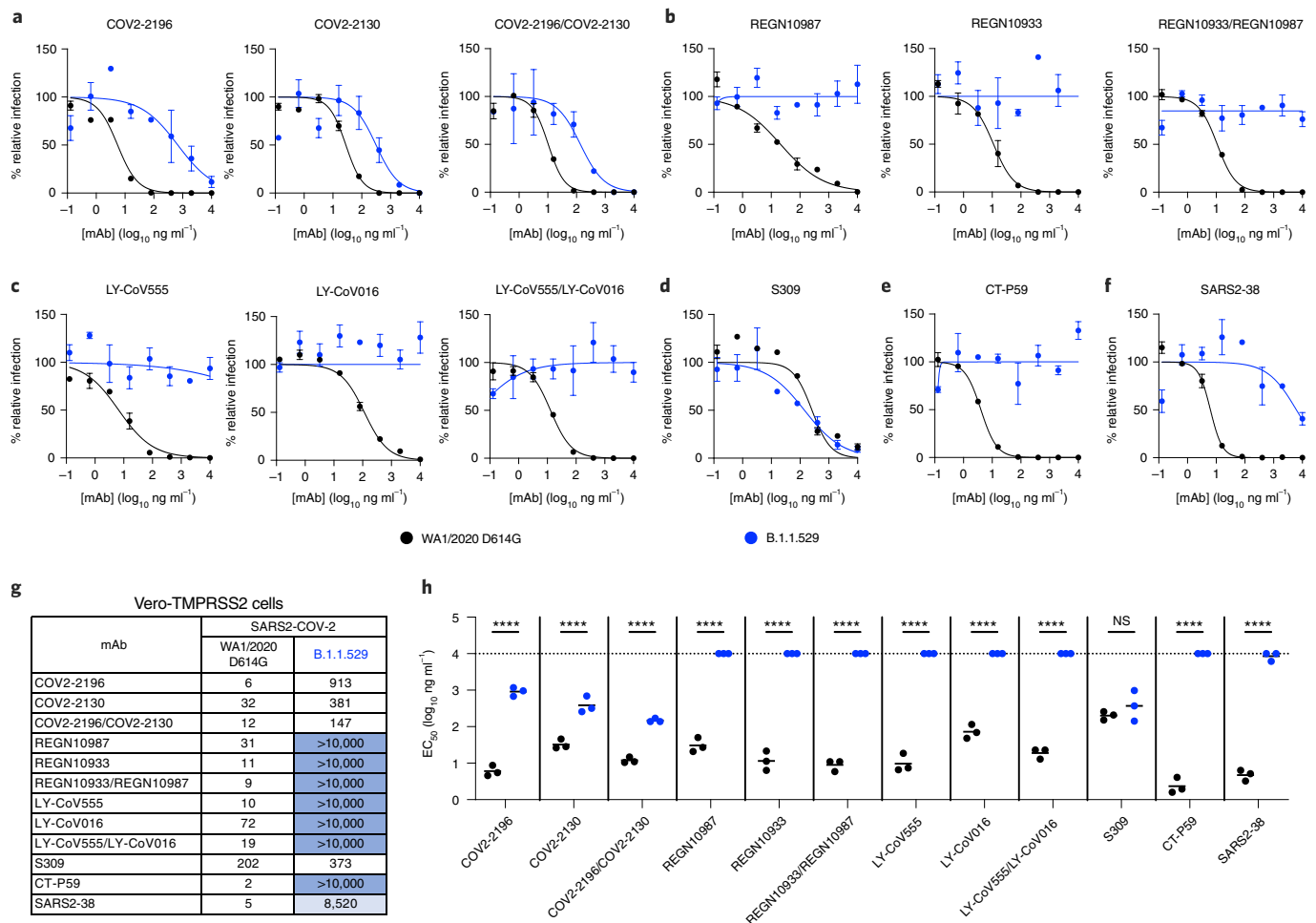
Fig. 2 | Neutralization of SARS-CoV-2 B.1.1.529 Omicron strain by mAbs in Vero-TMPRSS2 cells. a–f, Neutralization curves in Vero-TMPRSS2 cells comparing the sensitivity of SARS-CoV-2 strains with the indicated mAbs (COV2-2196, COV2-2130, REGN10933, REGN10987, LY-CoV555, LY-CoV016, S309, CT-P59 and SARS2-38) with WA1/2020 D614G and B.1.1.529. Also shown are the neutralization curves for antibody cocktails (COV2-2196/COV2-2130, REGN10933/REGN10987 or LY-CoV555/LY-CoV016). For data with mAb combinations, the x axis represents the total concentration of mAb used. One representative experiment of three performed in technical duplicate is shown. Error bars indicate the range of technical replicates. Data (% relative infection) are normalized to a no-mAb control. **g,** Summary of EC_{50} values (ng ml^{-1}) of neutralization of SARS-CoV-2 viruses (WA1/2020 D614G and B.1.1.529) performed in Vero-TMPRSS2 cells. Data are the geometric mean of three experiments. Blue shading: light, $EC_{50} > 5,000$ ng ml^{-1}; dark, $EC_{50} > 10,000$ ng ml^{-1}. **h,** Comparison of EC_{50} values by mAbs against WA1/2020 D614G and B.1.1.529 (three experiments; NS, not significant; ****$P < 0.0001$; two-way ANOVA with Sidak's post test). Each symbol represents neutralization data from an individual experiment. Bars indicate mean values. The dotted line indicates the upper limit of dosing of the assay.

Given the number of substitutions in the B.1.1.529 spike protein, including eight amino acid changes (K417N, G446S, S477N, Q493R, G496S, Q498R, N501Y and Y505H) in the ACE2 receptor-binding motif (RBM), we first evaluated possible effects on the structurally defined binding epitopes[12,13] of mAbs corresponding to those with EUA approval or in advanced clinical development (S309 (parent of VIR-7831 (sotrovimab)), RBD group III)[14,15]; COV2-2196 (RBD group I) and COV2-2130 (RBD group III) (parent mAbs of AZD8895 and AZD1061, respectively)[16]; REGN10933 (RBD group I) and REGN10987 (RBD group III)[17]; LY-CoV555 (RBD group I) and LY-CoV016 (RBD group I)[18,19]; and CT-P59 (Celltrion, RBD group I)[20], along with an additional broadly neutralizing mAb (SARS2-38 (RBD group II)) that we recently described[21]. We mapped the B.1.1.529 spike mutations onto the antibody-bound SARS-CoV-2 spike or RBD structures published in the RCSB Protein Data Bank (PDB) (Fig. 1c–k). Although every antibody analyzed had structurally defined recognition sites that were altered in the B.1.1.529 spike, the differences varied among mAbs, with some showing

larger numbers of changed residues (Fig. 1l: COV2-2196, n = 5; COV2-2130, n = 4; S309, n = 2; REGN10987, n = 4; REGN10933, n = 8; Ly-CoV555, n = 2; Ly-CoV016, n = 6; CT-P59, n = 8; and SARS2-38, n = 2).

To address the functional significance of the spike sequence variation in B.1.1.529 for antibody neutralization, we used a high-throughput focus reduction neutralization test (FRNT)[22] with WA1/2020 D614G and B.1.1.529 in Vero-TMPRSS2 cells (Fig. 2). We tested individual mAbs and combinations of mAbs that target the RBD in Vero-TMPRSS2 cells, including S309 (Vir Biotechnology); COV2-2130/COV2-2196 (parent mAbs of AZD1061 and AZD8895, provided by Vanderbilt University Medical Center); REGN10933/REGN10987 (synthesized based on casirivimab and imdevimab sequences from Regeneron); LY-CoV555/LY-CoV016 (synthesized based on bamlanivimab and etesevimab sequences from Eli Lilly); CT-P59 (synthesized based on regdanvimab sequences from Celltrion); and SARS2-38. As expected, all individual mAbs or combinations of mAbs tested neutralized the WA1/2020 D614G isolate,
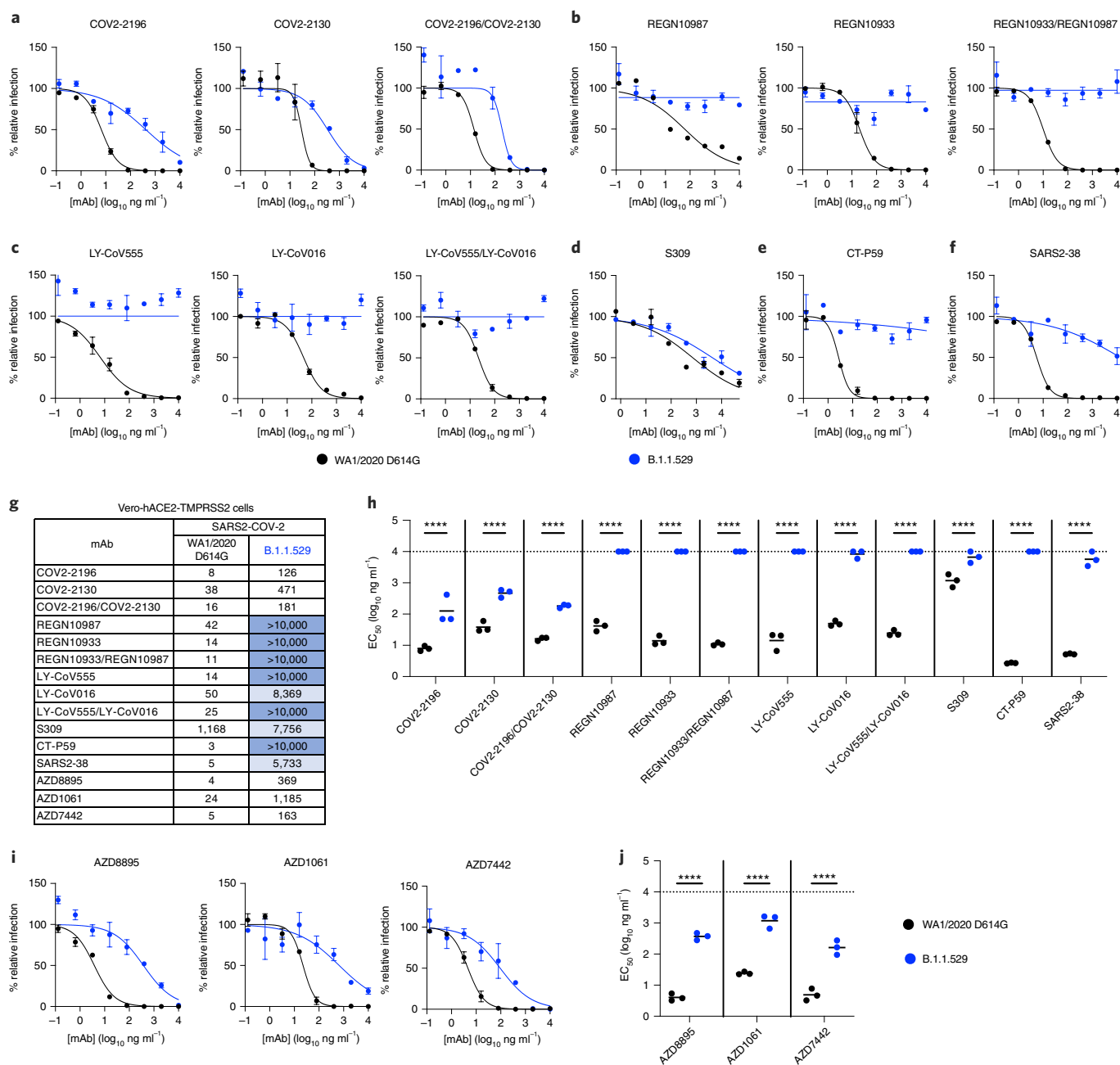
Fig. 3 | Neutralization of SARS-CoV-2 B.1.1.529 Omicron strain by mAbs in Vero-hACE2-TMPRSS2 cells. a–f, Neutralization curves in Vero-hACE2-TMPRSS2 cells comparing the sensitivity of SARS-CoV-2 strains with the indicated mAbs (S309, COV2-2196, COV2-2130, REGN10933, REGN10987, LY-CoV555, LY-CoV016, CT-P59 and SARS2-38) with WA1/2020 D614G and B.1.1.529. Also shown are the neutralization curves for antibody cocktails (COV2-2196/COV2-2130, REGN10933/REGN10987 or LY-CoV555/LY-CoV016). For data with mAb combinations, the *x* axis represents the total concentration of mAb used. One representative experiment of three performed in technical duplicate is shown. Error bars indicate range of technical replicates. Data (% relative infection) are normalized to a no-mAb control. **g**, Summary of EC_{50} values (ng ml^{-1}) of neutralization of SARS-CoV-2 viruses (WA1/2020 D614G and B.1.1.529) performed in Vero-hACE2-TMPRSS2 cells. Data are the geometric mean of three experiments. Blue shading: light, $EC_{50} > 5,000$ ng ml^{-1}; dark, $EC_{50} > 10,000$ ng ml^{-1}. **h**, Comparison of EC_{50} values by mAbs against WA1/2020 D614G and B.1.1.529. **i, j**, Neutralization curves in Vero-hACE2-TMPRSS2 cells comparing WA1/2020 D614G and B.1.1.529 infection in the presence of AZD1061, AZD8895 and the combination AZD7442. **h, j**, Three experiments; ****$P < 0.0001$; two-way ANOVA with Sidak's post test. Each symbol represents neutralization data from an individual experiment. Bars indicate mean values. The dotted line indicates the upper limit of dosing of the assay.

with half-maximal inhibitory concentration (EC_{50}) values similar to published data[6,20,23]. However, when tested alone, REGN10933, REGN10987, LY-CoV555, LV-CoV016, CT-P59 and SARS2-38 completely lost neutralizing activity against B.1.1.529, with little inhibitory capacity even at the highest (10,000 ng ml^{-1}) concentration

tested. COV2-2130 and COV2-2196 showed an intermediate ~12-fold and 150-fold ($P < 0.0001$) loss in inhibitory activity, respectively, against the B.1.1.529 strain. In comparison, S309 showed a less than two-fold ($P > 0.5$) reduction in neutralizing activity against B.1.1.529 (Fig. 2a–h). Analysis of mAb combinations currently in

clinical use showed that REGN10933/REGN10987 and LY-CoV555/LV-CoV016 lost all neutralizing activity against B.1.1.529, whereas COV2-2130/COV2-2196 showed a ~12-fold ($P < 0.0001$) reduction in inhibitory activity from an EC_{50} of 12 ng ml^{-1} to 147 ng ml^{-1}.

We repeated experiments in Vero-hACE2-TMPRSS2 cells to account for effects of hACE2 expression, which can affect neutralization by some anti-SARS-CoV-2 mAbs[21,24]. Moreover, modeling studies suggest that the mutations in the B.1.1.529 spike might enhance interactions with hACE2 (ref. [25]). All individual mAbs or combinations of mAbs tested neutralized the WA1/2020 D614G isolate as expected. However, REGN10933, REGN10987, LY-CoV555, LV-CoV016, SARS2-38 and CT-P59 completely lost neutralizing activity against B.1.1.529, and the combinations of REGN10933/REGN10987 or LY-CoV555/LV-CoV016 also lacked inhibitory capacity (Fig. 3a–h). In comparison, COV2-2130 and COV2-2196 showed reduced activity (~12-fold and 16-fold, respectively, $P < 0.0001$) against B.1.1.529, as did the combination of COV2-2130/COV2-2196 mAbs (~11-fold, $P < 0.0001$). The S309 mAb exhibited less potent neutralizing activity in Vero-hACE2-TMPRSS2 cells against WA1/2020 D614G virus with a flatter dose–response curve (Fig. 3d), as seen previously[6,26], and showed a moderate (~six-fold, $P < 0.0001$) reduction in neutralizing activity against B.1.1.529. Thus, although the trends in mAb neutralization of B.1.1.529 generally were similar to Vero-TMPRSS2 cells, some minor differences in potency were noted in cells expressing hACE2.

Discussion

Our experiments show a marked loss of inhibitory activity by several of the most highly neutralizing mAbs that are in advanced clinical development or have EUA approval. We evaluated antibodies that correspond to monotherapy or combination therapy that have shown pre- and post-exposure success in clinical trials and in patients infected with historical SARS-CoV-2 isolates. Our results confirm in silico predictions of how amino acid changes in B.1.1.529 RBD might negatively affect neutralizing antibody interactions[18,27]. Moreover, they agree with preliminary studies showing that several clinically used antibodies lose neutralizing activity against B.1.1.529 spike-expressing recombinant lentiviral or vesicular stomatitis virus (VSV)-based pseudoviruses[28–30]. One difference is that our study with authentic B.1.1.529 showed only moderately reduced neutralization by antibodies corresponding to the AstraZeneca combination (COV2-2196 and COV2-2130); in contrast, another group reported escape of these mAbs using a VSV pseudovirus displaying a B.1.1.529 spike protein in Huh7 hepatoma cells[29]. Additional studies are needed to determine whether this disparity in results is due to the cell type, the virus (authentic versus pseudotype) or preparation and combination of antibody. To begin to address this issue, we obtained AZD1061, AZD8895 and the combination AZD7442 directly from the manufacturer and tested them for neutralization of WA1/2020 D614G and B.1.1529 in Vero-hACE2-TMPRSS2 cells. We observed relatively similar reductions in inhibitory activity compared to the preclinical COV2-2130 and COV2-2196 mAbs with 49-, 92- and 33-fold lower EC_{50} values against B.1.1.529 by AZD1061, AZD8895 and AZD7442, respectively (Fig. 3g,i–j).

Although the Regeneron (REGN10933 and REGN10987), Eli Lilly (LY-CoV555 and LV-CoV016) and Celltrion (CT-P59) antibodies or combinations showed an almost complete loss of neutralizing activity against B.1.1.529, in our assays with Vero-TMPRSS2 and Vero-hACE2-TMPRSS2 cells the mAbs corresponding to the AstraZeneca combination (COV-2196 and COV-2130) or Vir Biotechnology (S309) products retained substantial inhibitory activity. Although these data suggest that some mAbs in clinical use might retain benefit, validation experiments in vivo[7] are needed to support this conclusion and inform clinical decisions.

Given the loss of inhibitory activity against B.1.1.529 of many highly neutralizing anti-RBD mAbs in our study, it appears

likely that serum polyclonal antibody responses generated after vaccination or natural infection also might lose substantial inhibitory activity against B.1.1.529, which could compromise protective immunity and explain a rise in symptomatic infections in vaccinated individuals[31]. Indeed, studies have reported approximately 25-fold to 40-fold reductions in serum neutralizing activity compared to historical D614G-containing strains from individuals immunized with the Pfizer BNT162b2 and AstraZeneca AZD1222 vaccines[28,30,32,33].

We note several limitations of our study. (1) Our experiments focused on the effect of the extensive sequence changes in the B.1.1.529 spike protein on mAb neutralization in cell culture. Despite observing differences in neutralizing activity with certain mAbs, it remains to be determined how this finding translates into effects on clinical protection against B.1.1.529. (2) Although virus neutralization is a correlate of immune protection against SARS-CoV-2 (refs. [7,34,35]), this measurement does not account for Fc effector functions if antibodies residually bind B.1.1.529 spike proteins on the virion or surface of infected cells. Fcγ receptor or complement protein engagement by spike-binding antibodies could confer substantial protection[36–38]. It should be noted that some antibodies have been engineered to have reduced Fc effector binding/function (e.g., the clinical antibodies AZD1061 and AZD8895). (3) We used the prevailing B.1.1.529 Omicron isolate that lacks an R346K mutation. Although only 8.3% of B.1.1.529 sequences in GISAID (accessed on 14 December 2021) have an R346K mutation, this substitution might further affect neutralization of some of the clinically used mAbs given that R346 is a contact residue for COV2-2130, REGN10987 and S309 (Fig. 1l). At least for S309, the R346K mutation did not affect neutralization of pseudoviruses displaying B.1.1.529 spike proteins[30]. Nonetheless, studies with infectious B.1.1.529 isolates with R346K mutations might be warranted if the substitution becomes more prevalent. (4) Our data are derived from experiments with Vero-TMPRSS2 and Vero-hACE2-TMPRSS2 cells. Although these cells standardly are used to measure antibody neutralization of SARS-CoV-2 strains, primary cells targeted by SARS-CoV-2 in vivo can express unique sets of attachment and entry factors[39], which could affect receptor and entry blockade by specific antibodies. Indeed, previous studies have reported that the cell line used can affect the potency of antibody neutralization against different SARS-CoV-2 variants[6].

In summary, our cell-culture-based analysis of neutralizing mAb activity against an authentic infectious B.1.1.529 Omicron SARS-CoV-2 isolate suggests that several, but not all, existing therapeutic antibodies will lose protective benefit. Thus, the continued identification and use of broadly and potently neutralizing mAbs that target the most highly conserved residues on the SARS-CoV-2 spike likely is needed to prevent resistance against B.1.1.529 and future variants with highly mutated spike sequences.

Online content

Any methods, additional references, Nature Research reporting summaries, source data, extended data, supplementary information, acknowledgements, peer review information; details of author contributions and competing interests; and statements of data and code availability are available at https://doi.org/10.1038/s41591-021-01678-y.

References

1. Sempowski, G. D., Saunders, K. O., Acharya, P., Wiehe, K. J. & Haynes, B. F. Pandemic preparedness: developing vaccines and therapeutic antibodies for COVID-19. *Cell* **181**, 1458–1463 (2020).
2. & Wibmer, C. K. et al. SARS-CoV-2 501Y.V2 escapes neutralization by South African COVID-19 donor plasma. *Nat. Med.* **27**, 622–625 (2021).

3. Wang, Z. et al. mRNA vaccine-elicited antibodies to SARS-CoV-2 and circulating variants. *Nature* **592**, 616–622 (2021).
4. Tada, T. et al. Neutralization of viruses with European, South African, and United States SARS-CoV-2 variant spike proteins by convalescent sera and BNT162b2 mRNA vaccine-elicited antibodies. Preprint at https://www.biorxiv.org/content/10.1101/2021.02.05.430003v1 (2021).
5. Wang, P. et al. Antibody resistance of SARS-CoV-2 variants B.1.351 and B.1.1.7. *Nature* **593**, 130–135 (2021).
6. Chen, R. E. et al. Resistance of SARS-CoV-2 variants to neutralization by monoclonal and serum-derived polyclonal antibodies. *Nat. Med.* **27**, 717–726 (2021).
7. Chen, R. E. et al. In vivo monoclonal antibody efficacy against SARS-CoV-2 variant strains. *Nature* **596**, 103–108 (2021).
8. Callaway, E. & Ledford, H. How bad is Omicron? What scientists know so far. *Nature* **600**, 197–199 (2021).
9. Torjesen, I. Covid-19: Omicron may be more transmissible than other variants and partly resistant to existing vaccines, scientists fear. *BMJ* **375**, n2943 (2021).
10. Johnson, B. A. et al. Loss of furin cleavage site attenuates SARS-CoV-2 pathogenesis. *Nature* **591**, 293–299 (2021).
11. Chen, J., Wang, R., Gilby, N. B. & Wei, G. W. Omicron (B.1.1.529): infectivity, vaccine breakthrough, and antibody resistance. Preprint at https://arxiv.org/abs/2112.01318 (2021).
12. Barnes, C. O. et al. SARS-CoV-2 neutralizing antibody structures inform therapeutic strategies. *Nature* **588**, 682–687 (2020).
13. Greaney, A. J. et al. Mapping mutations to the SARS-CoV-2 RBD that escape binding by different classes of antibodies. *Nat. Commun.* **12**, 4196 (2021).
14. Pinto, D. et al. Cross-neutralization of SARS-CoV-2 by a human monoclonal SARS-CoV antibody. *Nature* **583**, 290–295 (2020).
15. Gupta, A. et al. Early treatment for Covid-19 with SARS-CoV-2 neutralizing antibody sotrovimab. *N. Engl. J. Med.* **385**, 1941–1950 (2021).
16. Zost, S. J. et al. Potently neutralizing and protective human antibodies against SARS-CoV-2. *Nature* **584**, 443–449 (2020).
17. Baum, A. et al. REGN-COV2 antibodies prevent and treat SARS-CoV-2 infection in rhesus macaques and hamsters. *Science* **370**, 1110–1115 (2020).
18. Starr, T. N., Greaney, A. J., Dingens, A. S. & Bloom, J. D. Complete map of SARS-CoV-2 RBD mutations that escape the monoclonal antibody LY-CoV555 and its cocktail with LY-CoV016. *Cell Rep. Med.* **20**, 100255 (2021).
19. Gottlieb, R. L. et al. Effect of bamlanivimab as monotherapy or in combination with etesevimab on viral load in patients with mild to moderate COVID-19: a randomized clinical trial. *JAMA* **325**, 632–644 (2021).
20. Kim, C. et al. A therapeutic neutralizing antibody targeting receptor binding domain of SARS-CoV-2 spike protein. *Nat. Commun.* **12**, 288 (2021).
21. VanBlargan, L. A. et al. A potently neutralizing SARS-CoV-2 antibody inhibits variants of concern by utilizing unique binding residues in a highly conserved epitope. *Immunity* **54**, 2399–2416 (2021).
22. Case, J. B. et al. Neutralizing antibody and soluble ACE2 inhibition of a replication-competent VSV-SARS-CoV-2 and a clinical isolate of SARS-CoV-2. *Cell Host Microbe* **28**, 475–485 (2020).
23. Cathcart, A. L. et al. The dual function monoclonal antibodies VIR-7831 and VIR-7832 demonstrate potent in vitro and in vivo activity against SARS-CoV-2. Preprint at https://www.biorxiv.org/content/10.1101/2021.03.09.434607v8 (2021).
24. Suryadevara, N. et al. Neutralizing and protective human monoclonal antibodies recognizing the N-terminal domain of the SARS-CoV-2 spike protein. *Cell* **184**, 2316–2331 (2021).
25. Golcuk, M., Yildiz, A. & Gur, M. The Omicron variant increases the interactions of SARS-CoV-2 spike glycoprotein with ACE2. Preprint at https://www.biorxiv.org/content/10.1101/2021.12.06.471377v1 (2021).
26. Lempp, F. A. et al. Lectins enhance SARS-CoV-2 infection and influence neutralizing antibodies. *Nature* **598**, 342–347 (2021).
27. Ford, C. T., Machado, D. J. & Janies, D. A. Predictions of the SARS-CoV-2 Omicron variant (B.1.1.529) spike protein receptor-binding domain structure and neutralizing antibody interactions. Preprint at https://www.biorxiv.org/content/10.1101/2021.12.03.471024v3.full (2021).
28. Wilhelm, A. et al. Reduced neutralization of SARS-CoV-2 Omicron variant by vaccine sera and monoclonal antibodies. Preprint at https://www.medrxiv.org/content/10.1101/2021.12.07.21267432v1 (2021).
29. Cao, Y. R. et al. B.1.1.529 escapes the majority of SARS-CoV-2 neutralizing antibodies of diverse epitopes. Preprint at https://www.biorxiv.org/content/10.1101/2021.12.07.470392v1 (2021).
30. Cameroni, E. et al. Broadly neutralizing antibodies overcome SARS-CoV-2 Omicron antigenic shift. *Nature* https://doi.org/10.1038/d41586-021-03825-4 (2021).
31. Callaway, E. Omicron likely to weaken COVID vaccine protection. *Nature* **600**, 367–368 (2021).
32. Cele, S. et al. SARS-CoV-2 Omicron has extensive but incomplete escape of Pfizer BNT162b2 elicited neutralization and requires ACE2 for infection. Preprint at https://www.medrxiv.org/content/10.1101/2021.12.08.21267417v1 (2021).
33. Dejnirattisai, W. et al. Reduced neutralisation of SARS-COV-2 Omicron-B.1.1.529 variant by post-immunisation serum. Preprint at https://www.medrxiv.org/content/10.1101/2021.12.10.21267534v1 (2021).
34. Kim, J. H., Marks, F. & Clemens, J. D. Looking beyond COVID-19 vaccine phase 3 trials. *Nat. Med.* **27**, 205–211 (2021).
35. Khoury, D. S. et al. Neutralizing antibody levels are highly predictive of immune protection from symptomatic SARS-CoV-2 infection. *Nat. Med.* **27**, 1205–1211 (2021).
36. Schäfer, A. et al. Antibody potency, effector function, and combinations in protection and therapy for SARS-CoV-2 infection in vivo. *J. Exp. Med.* **218**, e20201993 (2021).
37. Zohar, T. et al. Compromised humoral functional evolution tracks with SARS-CoV-2 mortality. *Cell* **183**, 1508–1519 (2020).
38. Winkler, E. S. et al. Human neutralizing antibodies against SARS-CoV-2 require intact Fc effector functions for optimal therapeutic protection. *Cell* **184**, 1804–1820 (2021).
39. Bailey, A. L. & Diamond, M. S. A Crisp(r) new perspective on SARS-CoV-2 biology. *Cell* **184**, 15–17 (2021).
40. Lan, J. et al. Structure of the SARS-CoV-2 spike receptor-binding domain bound to the ACE2 receptor. *Nature* **581**, 215–220 (2020).

Methods

Cells. Vero-TMPRSS2 (ref. [41]) and Vero-hACE2-TMPRSS2 (ref. [6]) cells were cultured at 37 °C in DMEM supplemented with 10% FBS, 10 mM HEPES pH 7.3 and 100 U ml^{-1} of penicillin–streptomycin. Vero-TMPRSS2 cells were supplemented with 5 µg ml^{-1} of blasticidin. Vero-hACE2-TMPRSS2 cells were supplemented with 10 µg ml^{-1} of puromycin. All cells routinely tested negative for mycoplasma using a PCR-based assay.

Viruses. The WA1/2020 recombinant strain with substitutions (D614G) was described previously[42]. The B.1.1.529 isolate (hCoV-19/USA/WI-WSLH-221686/2021) was obtained from an individual in Wisconsin as a midturbinate nasal swab and passaged once on Vero-TMPRSS2 cells[43]. All viruses were subjected to next-generation sequencing (GISAID: EPI_ISL_7263803) to confirm the stability of substitutions. All virus experiments were performed in an approved Biosafety Level 3 facility.

Monoclonal antibody purification. The mAbs used in this study (COV2-2196, COV2-2130, S309, REGN10933, REGN10987, LY-CoV555, LY-CoV016, CT-P59, SARS2-38, AZD1061, AZD8895 and AZD7442) have been described previously[14,17,21,44–48]. S309 is the parent of VIR-7831 (sotrovimab); the clinically used mAb is engineered for enhanced clinical developability, as reported previously[23]. COV2-2196 and COV2-2130 mAbs were produced after transient transfection using the Gibco ExpiCHO Expression System (Thermo Fisher Scientific) following the manufacturer's protocol. Culture supernatants were purified using HiTrap MabSelect SuRe columns (Cytiva, formerly GE Healthcare Life Sciences) on an ÄKTA Pure chromatographer (GE Healthcare Life Sciences). Purified mAbs were buffer exchanged into PBS, concentrated using Amicon Ultra-4 50-kDa centrifugal filter units (Millipore Sigma) and stored at −80 °C until use. Purified mAbs were tested for endotoxin levels (found to be less than 30 endotoxin units (EU) per milligram IgG). Endotoxin testing was performed using the PTS201F cartridge (Charles River Laboratories), with a sensitivity range from 10 to 0.1 EU per milliliter, and an Endosafe Nexgen-MCS instrument (Charles River Laboratories). S309, REGN10933, REGN10987, LY-CoV016, LY-CoV555, CT-P59 and SARS2-38 mAb proteins were produced in CHOEXPI or EXPI293F cells and affinity purified using HiTrap Protein A columns (GE Healthcare, HiTrap mAb select Xtra no. 28-4082-61). Purified mAbs were suspended into 20 mM histidine, 8% sucrose pH 6.0 or PBS. The final products were sterilized by filtration through 0.22-µm filters and stored at 4 °C.

FRNT. Serial dilutions of mAbs were incubated with 10^2 focus-forming units of SARS-CoV-2 (WA1/2020 D614G or B.1.1.529) for 1 h at 37 °C. Antibody–virus complexes were added to Vero-TMPRSS2 or Vero-hACE2-TMPRSS2 cell monolayers in 96-well plates and incubated at 37 °C for 1 h. Subsequently, cells were overlaid with 1% (wt/vol) methylcellulose in MEM. Plates were harvested at 30 h (WA1/2020 D614G on Vero-TMPRSS2 cells), 70 h (B.1.1.529 on Vero-TMPRSS2 cells) or 24 h (both viruses on Vero-hACE2-TMPRSS2 cells) later by removal of overlays and fixation with 4% paraformaldehyde in PBS for 20 min at room temperature. A longer time of incubation was required for B.1.1.529-infected Vero-TMPRSS2 cells because the foci were smaller at the time point and difficult to quantitate. Plates with WA1/2020 D614G were washed and sequentially incubated with an oligoclonal pool (1 µg ml^{-1} of each) of SARS2-2, SARS2-11, SARS2-16, SARS2-31, SARS2-38, SARS2-57 and SARS2-71 (ref. [49]) anti-S antibodies. Plates with B.1.1.529 were additionally incubated with a pool of mAbs that cross-react with SARS-CoV-1 and bind a CR3022-competing epitope on the RBD[21]. All plates were subsequently stained with HRP-conjugated goat anti-mouse IgG (Sigma-Aldrich, A8924, 1:1,000) in PBS supplemented with 0.1% saponin and 0.1% BSA. SARS-CoV-2-infected cell foci were visualized by KPL TrueBlue peroxidase substrate and quantitated on an ImmunoSpot microanalyzer (Cellular Technologies). Data (% relative infection) are normalized to a no-mAb control. Antibody dose–response curves were analyzed using non-linear regression analysis with a variable slope (GraphPad Software), and the EC$_{50}$ was calculated.

Model of mAb-B.1.1.529 spike complexes. The spike model is a composite of data from PDB: 7C2L and PDB: 6W41. Models of mAb complexes were generated from their respective PDB files with the following accession codes: COV2-2196 (PDB: 7L7D); COV2-2130 (PDB: 7L7E); S309 (PDB: 6WPS); REGN10987 (PDB: 6XDG); REGN10933 (PDB: 6XDG); LY-CoV555 (PDB: 7KMG); LY-CoV016 (PDB: 7C01); CT-P59 (PDB: 7CM4); and SARS2-38 (PDB: 7MKM). Epitope footprints used in the multiple sequence alignment were determined using PISA interfacial analysis on the various mAb:RBD complexes[50]. Structural figures were generated using UCSF ChimeraX[51].

Reagent availability. All reagents described in this paper are available through material transfer agreements. AZD8895 and AZD1061 may be obtained from AstraZeneca for non-commercial internal research purposes under material transfer agreements upon reasonable request.

Statistical analysis. The number of independent experiments and technical replicates used are indicated in the relevant figure legends. A two-way ANOVA with Sidak's post test was used for comparisons of antibody potency between WA1/2020 D614G and B.1.1.59.

Reporting Summary. Further information on research design is available in the Nature Research Reporting Summary linked to this article.

Data availability
All data supporting the findings of this study are available within the paper, in the Source Data and from the corresponding author upon reasonable request. There are no restrictions in obtaining access to primary data. Source data are provided with this paper.

Code availability
No code was used in the course of the data acquisition or analysis.

References

41. Zang, R., et al. TMPRSS2 and TMPRSS4 promote SARS-CoV-2 infection of human small intestinal enterocytes. *Sci. Immunol.* **5**, eabc3582 (2020).
42. Plante, J. A. et al. Spike mutation D614G alters SARS-CoV-2 fitness. *Nature* **592**, 116–121 (2020).
43. Imai, M. et al. Syrian hamsters as a small animal model for SARS-CoV-2 infection and countermeasure development. *Proc. Natl Acad. Sci. USA* **117**, 16587–16595 (2020).
44. Zost, S. J. et al. Rapid isolation and profiling of a diverse panel of human monoclonal antibodies targeting the SARS-CoV-2 spike protein. *Nat. Med.* **26**, 1422–1427 (2020).
45. Tortorici, M. A. et al. Ultrapotent human antibodies protect against SARS-CoV-2 challenge via multiple mechanisms. *Science* **370**, 950–957 (2020).
46. Baum, A. et al. Antibody cocktail to SARS-CoV-2 spike protein prevents rapid mutational escape seen with individual antibodies. *Science* **369**, 1014–1018 (2020).
47. Jones, B. E. et al. The neutralizing antibody, LY-CoV555, protects against SARS-CoV-2 infection in nonhuman primates. *Sci. Trans. Med.* **13**, eabf1906 (2021).
48. Shi, R. et al. A human neutralizing antibody targets the receptor-binding site of SARS-CoV-2. *Nature* **584**, 120–124 (2020).
49. Liu, Z. et al. Identification of SARS-CoV-2 spike mutations that attenuate monoclonal and serum antibody neutralization. *Cell Host Microbe* **29**, 477–488 (2021).
50. Krissinel, E. & Henrick, K. Inference of macromolecular assemblies from crystalline state. *J. Mol. Biol.* **372**, 774–797 (2007).
51. Goddard, T. D. et al. UCSF ChimeraX: meeting modern challenges in visualization and analysis. *Protein Sci.* **27**, 14–25 (2018).

Author contributions
L.A.V. performed and analyzed neutralization assays. P.J.H. and L.A.V. propagated SARS-CoV-2 viruses. P.H. performed sequencing analysis. J.E.C., S.J.Z., L.P. and D.C. generated and provided mAbs. J.M.E. and D.H.F. performed structural analysis. J.E.C., D.H.F., Y.K. and M.S.D. obtained funding and supervised the research. L.A.V. and M.S.D. wrote the initial draft, with all other authors providing editorial comments.

Competing interests
M.S.D. is a consultant for Inbios, Vir Biotechnology, Senda Biosciences and Carnival Corporation and is on the Scientific Advisory Boards of Moderna and Immunome. The Diamond laboratory has received funding support in sponsored research agreements from Moderna, Vir Biotechnology and Emergent BioSolutions. J.E.C. has served as a consultant for Luna Biologics and Merck Sharp & Dohme, is on the Scientific Advisory Board of Meissa Vaccines and is the founder of IDBiologics. The Crowe laboratory has received sponsored research agreements from Takeda Vaccines, AstraZeneca and IDBiologics. Vanderbilt University has applied for patents related to two antibodies discussed in this paper. L.A.P. and D.C. are employees of Vir Biotechnology and may hold stock shares in Vir Biotechnology. L.A.P. is a former employee and shareholder in Regeneron Pharmaceuticals. The remaining authors declare no competing interests.

Additional information

nature portfolio

Corresponding author(s): Michael Diamond

Last updated by author(s): Dec 22, 2021

Reporting Summary

Nature Portfolio wishes to improve the reproducibility of the work that we publish. This form provides structure for consistency and transparency in reporting. For further information on Nature Portfolio policies, see our Editorial Policies and the Editorial Policy Checklist.

Statistics

For all statistical analyses, confirm that the following items are present in the figure legend, table legend, main text, or Methods section.

n/a	Confirmed	
☐	☒	The exact sample size (*n*) for each experimental group/condition, given as a discrete number and unit of measurement
☐	☒	A statement on whether measurements were taken from distinct samples or whether the same sample was measured repeatedly
☐	☒	The statistical test(s) used AND whether they are one- or two-sided *Only common tests should be described solely by name; describe more complex techniques in the Methods section.*
☒	☐	A description of all covariates tested
☒	☐	A description of any assumptions or corrections, such as tests of normality and adjustment for multiple comparisons
☐	☒	A full description of the statistical parameters including central tendency (e.g. means) or other basic estimates (e.g. regression coefficient) AND variation (e.g. standard deviation) or associated estimates of uncertainty (e.g. confidence intervals)
☐	☒	For null hypothesis testing, the test statistic (e.g. *F*, *t*, *r*) with confidence intervals, effect sizes, degrees of freedom and *P* value noted *Give P values as exact values whenever suitable.*
☒	☐	For Bayesian analysis, information on the choice of priors and Markov chain Monte Carlo settings
☒	☐	For hierarchical and complex designs, identification of the appropriate level for tests and full reporting of outcomes
☒	☐	Estimates of effect sizes (e.g. Cohen's *d*, Pearson's *r*), indicating how they were calculated

Our web collection on statistics for biologists contains articles on many of the points above.

Software and code

Policy information about availability of computer code

Data collection	No software was used in this study to collect data
Data analysis	Prism 8.0 was used to perform all data analysis. Structural figures were generated from publicly available data (Protein Data Base) using UCSF ChimeraX.

For manuscripts utilizing custom algorithms or software that are central to the research but not yet described in published literature, software must be made available to editors and reviewers. We strongly encourage code deposition in a community repository (e.g. GitHub). See the Nature Portfolio guidelines for submitting code & software for further information.

Data

Policy information about availability of data

All manuscripts must include a data availability statement. This statement should provide the following information, where applicable:
- Accession codes, unique identifiers, or web links for publicly available datasets
- A description of any restrictions on data availability
- For clinical datasets or third party data, please ensure that the statement adheres to our policy

All data supporting the findings of this study are available within the paper, in the Source Data, and from the corresponding author upon request. There are no restrictions in obtaining access to primary data. Models of mAb complexes were generated from their respective PDB files with the following accession codes: COV2-2196 (PDB: 7L7D); COV2-2130 (PDB: 7L7E); S309 (PDB: 6WPS); REGN-10987 (PDB: 6XDG); REGN-10933 (PDB: 6XDG)); LY-CoV555 (PDB: 7KMG) LY-CoV016 (PDB: 7C01); CT-P59 (PDB: 7CM4) and SARS2-38 (PDB: 7MKM).

Field-specific reporting

Please select the one below that is the best fit for your research. If you are not sure, read the appropriate sections before making your selection.

☒ Life sciences   ☐ Behavioural & social sciences   ☐ Ecological, evolutionary & environmental sciences

For a reference copy of the document with all sections, see nature.com/documents/nr-reporting-summary-flat.pdf

Life sciences study design

All studies must disclose on these points even when the disclosure is negative.

Sample size	No sample sizes were chosen a priori. All experiments were repeated at least three independent times, each with multiple technical replicates. Sample sizes were selected based on prior neutralization experiments with monoclonal antibodies and the ability to assess for loss of activuty
Data exclusions	No data was excluded.
Replication	All experiments had three biological and with each experiment two technical replicates were performed.
Randomization	No randomization was performed. This was not relevant to our in vitro study.
Blinding	No blinding was performed during the experimental set up phase (for convenience), although the data analysis was performed in a blinded manner

Reporting for specific materials, systems and methods

We require information from authors about some types of materials, experimental systems and methods used in many studies. Here, indicate whether each material, system or method listed is relevant to your study. If you are not sure if a list item applies to your research, read the appropriate section before selecting a response.

Materials & experimental systems

n/a	Involved in the study
☐	☒ Antibodies
☐	☒ Eukaryotic cell lines
☒	☐ Palaeontology and archaeology
☒	☐ Animals and other organisms
☒	☐ Human research participants
☒	☐ Clinical data
☒	☐ Dual use research of concern

Methods

n/a	Involved in the study
☒	☐ ChIP-seq
☒	☐ Flow cytometry
☒	☐ MRI-based neuroimaging

Antibodies

Antibodies used	Human mAbs: COV2-2196, COV2-2130, S309, REGN10933, REGN10987, LY-CoV555, LY-CoV016, CT-P59, AZD7442, AZD8895, and AZD1061. Mouse mAbs: SARS2-2, SARS2-11, SARS2-16, SARS2-31, SARS2-38, SARS2-57, and SARS2-71 (mouse mAbs from the Diamond laboratiry); HRP-conjugated goat anti-mouse IgG (Sigma, A8924, 1:1000)
Validation	All primary mAbs were validated using purified SARS-CoV-2 RBD or S proteins using an ELISA. All secondary antibodies were validated by each respective manufacturer per their associated DataSheets.

Eukaryotic cell lines

Policy information about cell lines

Cell line source(s)	Vero-TMPRSS2, Diamond laboratory; Vero-hACE2-TMPRSS2, Graham laboratory, VRC/NIH; Expi-CHO (ThermoFisher, A29127), Expi 293F (ThermoFisher, A14527)
Authentication	These cells grew as expected and propagated SARS-CoV-2 as expected. In addition, flow cytometry was used to confirm exoression of the transgenes.
Mycoplasma contamination	All cell lines are routinely tested each month and were negative for mycoplasma.
Commonly misidentified lines (See ICLAC register)	This study did not involve any commonly misidentified cell lines.